Hue University Journal of Science: Natural Science
Vol. 130, No. 1D, 55–64, 2021

pISSN 1859-1388
eISSN 2615-9678

DISPERSION AND NONLINEARITY PROPERTIES OF SMALL SOLID-CORE PHOTONIC FIBERS WITH As_2Se_3 SUBSTRATE

Thuy Nguyen Thi[1]*, Duc Hoang Trong[1], Tran Tran Bao Le[2], Trong Dang Van[2], Lanh Chu Van[2]

[1] University of Education, Hue University, 34 Le Loi St., Hue city, Viet Nam
[2] Department of Physics, Vinh University, 182 Le Duan St., Vinh city, Viet Nam

* Corresponding author: Thuy Nguyen Thi <ntthuy@hueuni.edu.vn>

(*Received: 21 June 2021; Accepted: 18 November 2021*)

Abstract. Characteristics of As_2Se_3 photonic crystal fibers (PCFs) with a solid-core and small-core diameter are numerically investigated in the long-wavelength range (from 2 to 10 μm). A full modal analysis and optical properties of designed photonic crystal fibers with lattice constant Λ and filling factor d/Λ are presented in terms of chromatic dispersion, effective refractive index, nonlinear coefficients, and confinement loss. The simulation results show that a high nonlinear coefficient of 4410.303 $W^{-1}{\cdot}km^{-1}$ and a low confinement loss of 10^{-20} $dB{\cdot}km^{-1}$ can simultaneously be achieved in the proposed PCFs at a 4.5 μm wavelength. Chromatic dispersions are flat. The values of dispersion increase with increasing filling factor d/Λ and decrease with the increase in lattice constant Λ. In particular, some chromatic dispersion curves also cut the zero-dispersion line at two points. The flat dispersion feature, high nonlinearity, and small confinement loss of the proposed photonic crystal fiber structure make it suitable for supercontinuum.

Keywords: Small solid-core photonic crystal fibers, chromatic dispersion, effective refractive index, confinement loss, nonlinear coefficient, nonlinear properties

1 Introduction

Photonic crystal fibers (PCFs) [1, 2] have recently gained attention because of their distinctive and unique properties that conventional optical fibers do not exhibit. Usually, PCFs are created with a periodic air holes structure along its length and a single core with silica glass. By skillfully arranging the structure, researchers are able to design the fibers, which have the desired transmission properties and interesting optical properties like single-mode operation in the wide wavelength range, wideband dispersion, large mode area, high birefringence, very high and low nonlinearity, excitation of nonlinear effects at a small mode area, flattened characteristics and manageable dispersion properties [3-10], endlessly single-mode guiding [11, 12], fiber sensors [13, 14], and fiber lasers [15, 16]. Although silica PCFs have extensively been studied with numerous advantages, silica has a weak nonlinear index. More importantly, any optical applications of silica PCFs should not exceed the limit of 2 μm of wavelength because of their intrinsic losses [17-21]. Therefore, non-silica glass PCFs must be expected to enhance the application of microstructured optical fibers. Some glasses, such as chalcogenide glasses, bismuth, tellurite, or lead silicate glasses, are very attractive because of their nonlinear properties. They have a higher nonlinear index than fused silica [22]. Among them, chalcogenide glasses exhibit the strongest glass nonlinearities (typically 500 times stronger than traditional silica glasses [23]). Designing an optical fiber with high nonlinearity, negative dispersion, and large birefringence is a continuous challenge for researchers. In addition, maximizing the bandwidth for the

supercontinuum generation also plays a significant role in the applications of this group of materials. Currently, numerous studies have demonstrated that nonlinear coefficients change drastically, and the zero-dispersion wavelength of optical fibers shifts towards longer wavelengths in the range of 4–5 μm by designing different structures of As_2Se_3-based PCFs. Furthermore, As_2Se_3-based PCFs are preferable to silica in fabricating fibers because of low softening temperature [24-35].

In practice, the characteristic solid-core As_2Se_3-based PCFs were fabricated in the wavelength range from 2 to 5 μm [28-37]. PCFs with lattice constants less than 3 μm were prepared to enhance birefringence and nonlinearity. In this paper, we studied highly nonlinear solid-core chalcogenide glass-based PCFs with a small-core diameter. We used As_2Se_3 as a host material to ensure high nonlinearity in the wide wavelength region from 2 to 10 μm. The chromatic dispersion and nonlinear properties of As_2Se_3-based PCFs were thoroughly analyzed by considering the effects of all the main design parameters, including the lattice constant Λ and filling factor d/Λ. The filling factor d/Λ was chosen in range of 0.3–0.85; lattice constant Λ = 3.0 μm and Λ = 3.5 μm.

2 Modeling and theory

Taking the nonlinearity into account, we designed PCFs with small-core diameters. The diameter of the core was determined with the formula $D_c = 2\Lambda - d$, showing the relationship among core diameter D_c, lattice constant Λ, and the diameter of air holes d. The schematic cross-section geometrical structure of As_2Se_3-based PCFs in conventional regular hexagonal lattices is shown in Fig. 1.

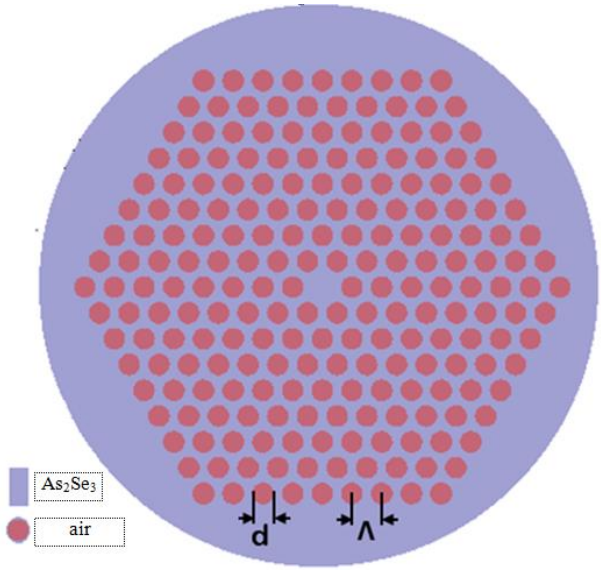

Fig. 1. Geometrical structure of PCFs with hexagonal As_2Se_3 substrate

The design with empty air holes consists of eight rings of air holes. The lattice constant Λ was fixed at 3.0 and 3.5 μm, and the filling factor d/Λ was chosen in a range of 0.3–0.85. With such design parameters, light is confined in the core (Fig. 2).

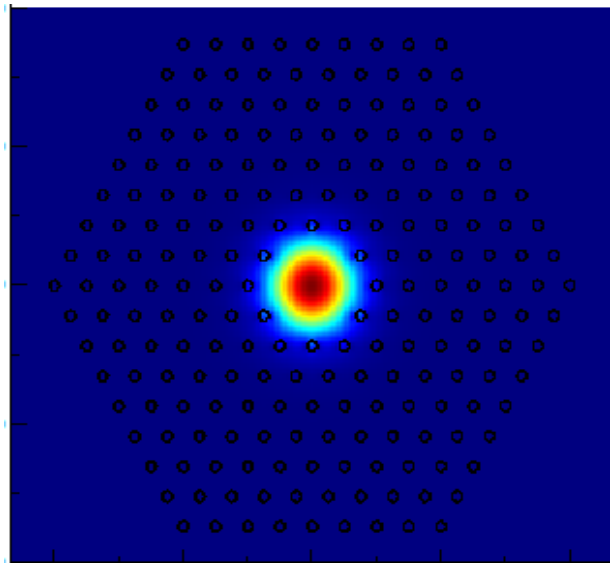

Fig. 2. Typical geometrical structure of PCFs and light confined in the core

pISSN 1859-1388
eISSN 2615-9678

To investigate the influence of structural parameters on the characteristic properties of PCFs, we used the commercial software Lumerical Model Solution multiphysics. Mathematically, the Maxwell equation was solved with the finite difference method. In addition, the mode profiles associated with the eigenvectors and the propagation constants corresponding to the eigenvalues are calculated [36].

The chromatic dispersion coefficient (D) of the PCFs was calculated from the n_{eff} values versus the wavelength (Eq. 1)

$$D = -\frac{\lambda}{c}\frac{d^2\,\mathrm{Re}\left[n_{\mathrm{eff}}\right]}{d\lambda^2} \quad (1)$$

where $\mathrm{Re}\left[n_{\mathrm{eff}}\right]$ is the real part of n_{eff}, which is the effective index of the guided mode calculated with the finite difference method, and c is the light speed in vacuum. The refractive index of modes was plotted as a function of wavelength. The refractive index of As_2Se_3 substrate was calculated according to Sellmeier's [37].

$$n^2 - 1 = \frac{2.234921\lambda^2}{\lambda^2 - 0.24164^2} + \frac{0.347441\lambda^2}{\lambda^2 - 19^2} + \frac{1.308575\lambda^2}{\lambda^2 - 4\times 0.24164^2} \quad (2)$$

The confinement loss (L_c) is also an important parameter to design PCFs with a finite number of air holes. L_c was created from the leaky mode and the photonic crystal fiber structure [33]. It can be calculated according to Eq. 3

$$L_c = 8.686 k_0\,\mathrm{Im}\left[n_{\mathrm{eff}}\right](dB) \quad (3)$$

where $\mathrm{Im}\left[n_{\mathrm{eff}}\right]$ is the imaginary part of the "n_{eff}" [34].

The nonlinear coefficient $\gamma(\lambda)$ of PCFs, which depends on the design of cladding structure parameters, can be determined following Eq. 4

$$\gamma(\lambda) = 2\pi n_2 / \left(\lambda A_{\mathrm{eff}}\right) \quad (4)$$

where n_2 is the nonlinear index of As_2Se_3 $\left(n_2 = 2.4\times 10^{-17}\ m^2.\mathrm{W}^{-1}\right)$ and A_{eff} is the model effective area. A_{eff} is a nonlinearity characteristic of a PCF and defined as [31]

$$A_{\mathrm{eff}} = \frac{\left(\int_{-\infty}^{\infty}\int_{-\infty}^{\infty}|E|^2\,dxdy\right)^2}{\int_{-\infty}^{\infty}\int_{-\infty}^{\infty}|E|^4\,dxdy} \quad (5)$$

In addition, the characteristics of PCFs can be flexibly controlled by adjusting the hole diameter and the lattice constant of the air hole arrays in the cladding. Usually, these properties depend strongly on the lattice constant Λ and the filling factor d/Λ.

3 Simulation results and analysis

3.1 Effective refraction index

The effective refraction index decreases with increasing wavelength and changes with varying lattice constant Λ and filling factor d/Λ; when d/Λ increases, the effective refraction index decreases. As shown in Fig. 3a and Fig. 3b, the longer wavelength is (5–10 μm), the more separated the curves are. The curves in Fig. 3a (Λ = 3.0 μm) are more separated than the others.

The values of the effective refractive index of fibers with various d/Λ and Λ at the 4.5 μm wavelength (expected to be a compatible pump wavelength for supercontinuum generation) are shown in Table 1a and Table 1b. When the lattice constant Λ increases, the effective refractive index also increases, and the maximum effective refractive index has a value of 2.0903 when Λ = 3.5 μm and d/Λ = 0.3. When the fiber with a smaller core (Λ = 3.0 μm and d/Λ = 0.3) has a smaller lattice constant, the difference between the two effective refractive index values for both cases is about 0.06.

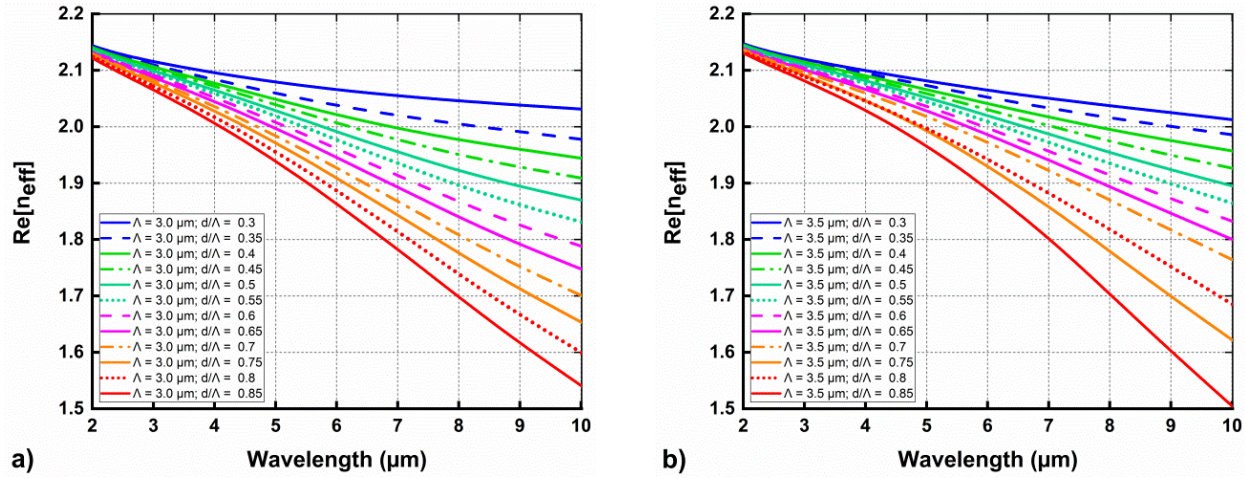

Fig. 3. The real part of effective refraction index as a function of wavelength of fibers with various d/Λ when Λ = 3.0 μm (a) and Λ = 3.5 μm (b)

Table 1. a. Effective refractive index of fibers with various d/Λ when Λ = 3.0 μm at 4.5 μm wavelength

d/Λ	0.3	0.35	0.4	0.45	0.5	0.55	0.6	0.65	0.7	0.75	0.8	0.85
Re [n_{eff}]	2.0872	2.0714	2.0628	2.0555	2.0469	2.0392	2.0303	2.0213	2.0105	2.0003	1.9871	1.9736

Table 1. b. Effective refractive index of fibers with various d/Λ when Λ = 3.5 μm at 4.5 μm wavelength

d/Λ	0.3	0.35	0.4	0.45	0.5	0.55	0.6	0.65	0.7	0.75	0.8	0.85
Re [n_{eff}]	2.0903	2.0839	2.0782	2.0725	2.0669	2.0608	2.0542	2.0476	2.0395	2.0208	2.0221	1.9987

3.2 Chromatic dispersion

Fig. 4a and Fig. 4b show the effect of changing filling factor d/Λ on chromatic dispersion (D) when Λ is 3.0 and 3.5 μm. An increase in d/Λ eventually increases the value of dispersion. It is obvious that flattened dispersion is greatly dependent on the ratio of d/Λ, and the peak of the D curve shifts towards longer wavelengths. In most cases, the chromatic dispersion curves intersect the zero-dispersion line at one or more points, except for the case when Λ = 3.0 μm, where the dispersion is completely located in the normal dispersion with a small value of the filling factor (d/Λ = 0.3). However, when the Λ value is greater, the chromatic dispersion curve with Λ and d/Λ being 3.5 μm and 0.3 has anomalous dispersion in the IR long-wavelength range with λ greater than 8.5 μm. The slope of the dispersion curves increases when the values of Λ increase, and the greater the dispersion slope is, the larger d/Λ is found. Thus, the slope depends strongly on the values of Λ and d/Λ. The chromatic dispersion curves are similar and flat in all cases, and the D curves are clearly separated from each other when they cross the zero-dispersion line. Note that we achieve high negative dispersion when the filling factor is in the range of 0.3–0.5 for both values of Λ. This is because the core dimension reduces when we increase the size of the air hole, resulting in a high field confinement. In telecommunication, negative chromatic dispersion is useful in

pISSN 1859-1388
eISSN 2615-9678

compensating the opposite slope dispersion to make the net dispersion of two fibers in the series become zero. In dispersion-compensating fibers, larger dispersion is compensated by a short length of the optical fiber with high negative dispersion [31]. Negative dispersion is obtained over a broad wavelength range because of the significant index difference between the core and the cladding. In PCFs, a considerable index difference can be easily obtained because it depends strongly on the cladding parameter, the filling factor d/Λ, and the achieved lattice constant Λ [31-37]. Because dispersion is one of the main factors for supercontinuum generation, the PCF with flat dispersion allows further broad supercontinuum generation. Thus, the goal of optimization of dispersion herein is to show the fiber structures with a flat near-zero dispersion shape and the zero dispersion wavelength (ZDW) compatible with the pump wavelength. Thus, it is possible to choose optimal designs when Λ is 3.0 and 3.5 μm, and d/Λ varies from 0.3 to 0.5, which is well suited for supercontinuum generation.

Table 2a and Table 2b show the dispersion values for all cases at the 4.5 μm wavelength. As seen in Table 2, the D value decreases with increasing Λ. The lowest and highest dispersion of 5.8272 ps·(nm·km)$^{-1}$ (Λ = 3.5 μm; d/Λ = 0.35) and 128.252 ps·(nm·km)$^{-1}$ (Λ = 3.0 μm; d/Λ = 0.85) can be obtained. At the 4.5 μm wavelength, when the lattice constant is equal to 3.0 μm, there are three negative D values. When the value of the lattice constant increases to 3.5 μm, there are also two negative D values. However, the negative D values were observed more in the range of investigated wavelength.

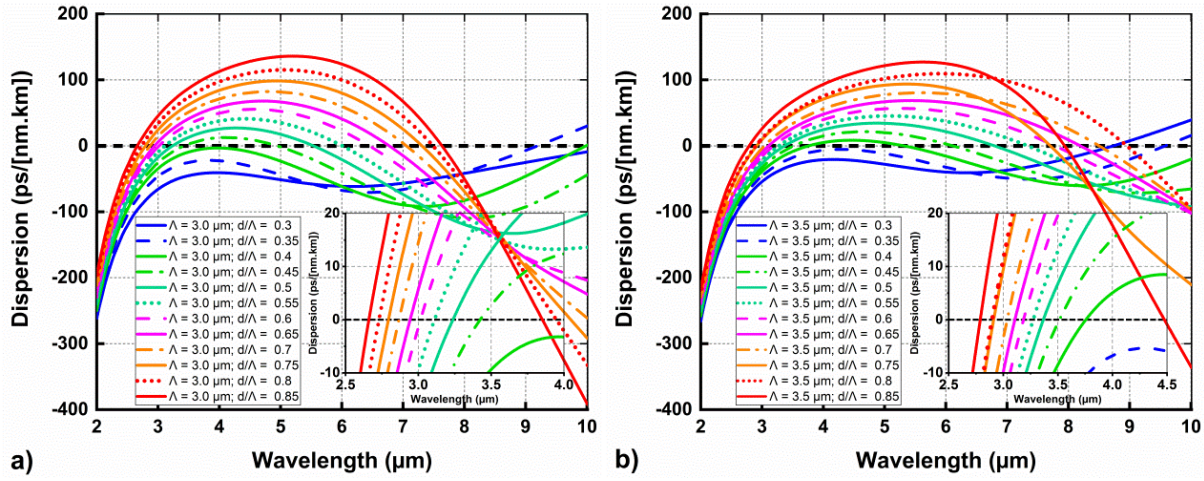

Fig. 4. Chromatic dispersion as a function of wavelength of fibers with various d/Λ when Λ = 3.0 μm (a) and Λ = 3.5 μm (b)

Table 2. a. Chromatic dispersion values of fibers with various d/Λ when Λ = 3.0 μm at 4.5 μm wavelength (ps·(nm·km)$^{-1}$)

d/Λ	0.3	0.35	0.4	0.45	0.5	0.55	0.6	0.65	0.7	0.75	0.8	0.85
D	–44.4237	–30.4944	–8.9780	10.0626	26.3277	41.0788	55.6294	67.4288	80.9254	95.5375	110.4967	128.2520

Table 2. b. Chromatic dispersion values of fibers with various d/Λ when Λ = 3.5 μm at 4.5 μm wavelength (ps·(nm·km)$^{-1}$)

d/Λ	0.3	0.35	0.4	0.45	0.5	0.55	0.6	0.65	0.7	0.75	0.8	0.85
D	–22.0857	–5.8272	8.6318	21.2794	32.7627	41.9906	51.1911	60.4237	69.7775	84.7853	91.5521	110.6829

The unique feature in small-core solid structures of these PCFs is that the *D* curves intersect the zero-dispersion line at several points. That means that there are multiple negative D values in different wavelength regions. The zero dispersion wavelengths calculated according to the variation of d/Λ and Λ of PCFs in the near-infrared range are shown in Table 3. It can be observed that different ZDW values depend on d/Λ and Λ. When Λ = 3.0 μm and d/Λ = 0.3, we cannot find the ZDW value because the dispersion curve does not intersect the zero-dispersion line, but when d/Λ increases, we have one and two ZDW values. Thus, the increase or decrease of chromatic dispersion depends strongly on the value of d/Λ and Λ. When Λ = 3.5 μm and d/Λ varies from 0.5 to 0.85, the dispersion curve intersects the zero-dispersion line at two points corresponding to two ZDW values. Multiple values of ZDW are in the long-wavelength region, which is very convenient for the supercontinuum generation in the infrared region.

Table 3. Zero dispersion wavelengths of fibers with various d/Λ and Λ

ZDW (μm)	Λ = 3.0 μm	Λ = 3.5 μm	ZDW (μm)	Λ = 3.0 μm	Λ = 3.5 μm
d/Λ = 0.3	–	8.7387	d/Λ = 0.6	3.0154 and 6.4595	3.1859 and 7.7956
d/Λ = 0.35	9.1945	9.5775	d/Λ = 0.65	2.9433 and 6.7796	3.1086 and 8.2138
d/Λ = 0.4	9.9791	3.7526 and 5.3226	d/Λ = 0.7	2.8656 and 7.0706	3.0375 and 8.5156
d/Λ = 0.45	3.4225 and 4.9563	3.5092 and 6.1276	d/Λ = 0.75	2.7925 and 7.3127	2.912 and 7.7285
d/Λ = 0.5	3.2378 and 5.5446	3.3675 and 6.799	d/Λ = 0.8	2.7284 and 7.4988	2.8971 and 8.982
d/Λ = 0.55	3.1133 and 6.0136	3.2727 and 7.3382	d/Λ = 0.85	2.6631 and 7.6642	2.7878 and 7.952

3.3 Effective nonlinearity

Nonlinearity is an important parameter for the calculation of different nonlinearities of PCFs. Because we used As_2Se_3 as a highly nonlinear chalcogenide material and designed small-core PCFs, we expected that the fibers would show higher nonlinearity. Fig. 5a and Fig. 5b show the effects of variation in wavelength, d/Λ, and Λ on the nonlinear coefficient γ. Increasing wavelength decreases nonlinearity, and a higher value of γ is found at shorter wavelengths. The smaller the value of Λ is, the higher the value of γ, but γ increases with increasing d/Λ at specified lattice constant values. For different d/Λ and Λ, the graph of γ is quite similar. As shown in Eq. 4, the nonlinear coefficient is inversely proportional to the model effective area (A_{eff}). With increasing d/Λ, the value of γ increases, so A_{eff} decreases accordingly. Several optimal structures, shown above when Λ is 3.0 and 3.5 μm, and d/Λ varies from 0.3 to 0.5, have relatively high nonlinear coefficients.

The nonlinear coefficients of the fiber with various d/Λ and Λ at the 4.5 μm wavelength are depicted in Table 4a and Table 4b. The maximum value of γ (4410.303 $W^{-1}{\cdot}km^{-1}$) appears when d/Λ is 0.85 and Λ is 0.3 μm (Tab. 4a). At the same time, the minimum value of γ is 799.028 $W^{-1}{\cdot}km^{-1}$ when d/Λ = 0.3 and Λ = 3.5 μm (Tab. 4b).

pISSN 1859-1388
eISSN 2615-9678

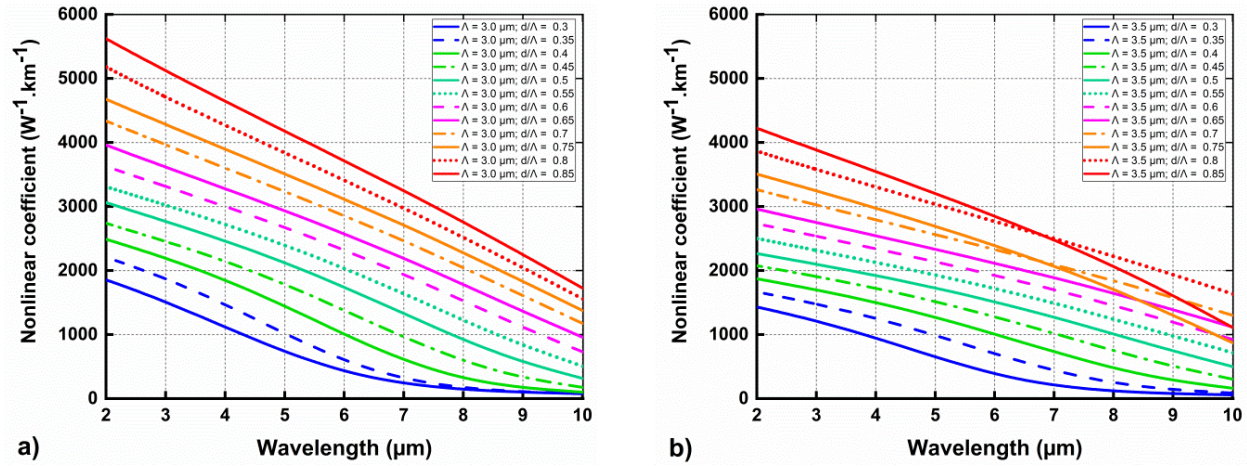

Fig. 5. Nonlinear coefficient as a function of wavelength of fibers with various d/Λ when Λ = 3.0 μm (a) and Λ = 3.5 μm (b)

Table 4. a. Nonlinear coefficient of fibers with various d/Λ and Λ = 3.0 μm at 4.5 μm wavelength ($W^{-1}{\cdot}km^{-1}$)

d/Λ	0.3	0.35	0.4	0.45	0.5	0.55	0.6	0.65	0.7	0.75	0.8	0.85
γ	923.427	1244.162	1652.145	1969.769	2295.239	2560.912	2838.678	3107.102	3417.724	3702.999	4054.157	4410.303

Table 4. b. Nonlinear coefficient of fibers with various d/Λ and Λ = 3.5 μm at 4.5 μm wavelength ($W^{-1}{\cdot}km^{-1}$)

d/Λ	0.3	0.35	0.4	0.45	0.5	0.55	0.6	0.65	0.7	0.75	0.8	0.85
γ	799.028	1124.048	1388.703	1621.900	1826.386	2029.653	2239.996	2437.794	2677.734	2834.230	3170.587	3375.573

3.4 Confinement loss

Fig. 6a and Fig. 6b present the confinement loss (L_c) as a function of wavelength of PCFs with various d/Λ and Λ. Its values increase with the wavelength and decrease quickly with the filling factor and lattice constant. It can be seen that the confinement loss is minimal because a small fraction of the total power is travelling through the air holes while most of the power is tightly confined in the small solid core. Especially when d/Λ equals 0.7 μm with Λ being 0.35, the value of confinement loss is minimal, and the curves almost coincide. The smallest confinement loss is 4.0013×10^{-20} dB/m when Λ = 3.5 μm and d/Λ = 0.7.

The confinement loss of PCFs with various d/Λ and Λ at the 3 and 4.5 μm wavelength is presented in Table 5a and Table 5b. Its value decreases with d/Λ and Λ of the air holes because of the decrease of absorption ability. When d/Λ is greater than 0.5, the value of confinement loss is minimal and similar. In addition, the highest value of confinement loss is 1.2288 dB/m when d/Λ = 0.3 and Λ = 3.0 μm.

Table 5. a. Confinement loss of fibers with various d/Λ when Λ = 3.0 μm at 4.5 μm wavelength (dB/m)

d/Λ	0.3	0.35	0.4	0.45	0.5	0.55	0.6	0.65	0.7	0.75	0.8	0.85
L_c	1.23E–00	4.99E–02	6.46E–04	4.82E–06	2.13E–08	8.95E–11	2.52E–13	3.92E–16	7.55E–19	3.70E–19	–220E–19	1.18E–18

Table 5. b. Confinement loss of fibers with various d/Λ when Λ = 3.5 μm at 4.5 μm wavelength (dB/m)

d/Λ	0.3	0.35	0.4	0.45	0.5	0.55	0.6	0.65	0.7	0.75	0.8	0.85
L_c	4.50E–01	6.58E–03	6.87E–05	5.85E–07	4.68E–09	2.24E–11	5.44E–14	1.054E–16	4.004E–20	–2.23E–19	–1.76E–19	1.01E–18

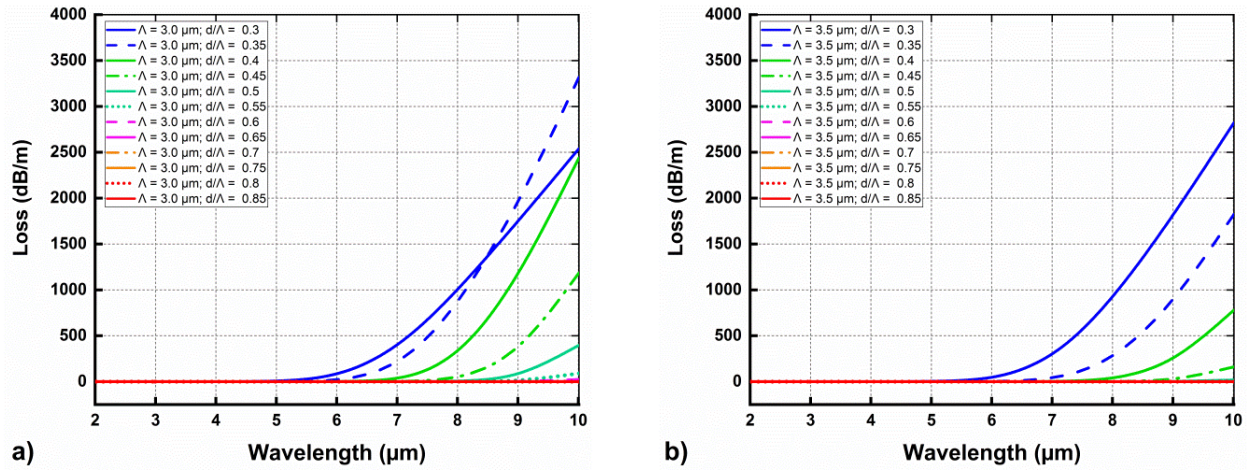

Fig. 6. Confinement loss as a function of wavelength of fibers with various d/Λ when Λ = 3.0 μm (a) and Λ = 3.5 μm (b)

4 Conclusion

In this work, the dispersion and nonlinearity of PCFs with As_2Se_3 small core are analyzed considering the effect of a new design parameter: the filling factor d/Λ and lattice constant Λ. The wavelengths of 4.5 μm in the infrared spectrum, convenient for super supercontinuum generation, are chosen to calculate the values of characteristic quantities. For smaller d/Λ and Λ values, flattened dispersion is observed. The chromatic dispersion curves intersect the zero-dispersion line at multiple points in different wavelength regions. The nearest chromatic dispersion to the zero-dispersion curve is observed when d/Λ = 0.3 and Λ = 3.0 μm. At the same time, the confinement loss of PCFs is minimal, at about 10^{-20} dB/m, and its curves almost coincide. Besides, the higher value of nonlinear coefficient is found at lower wavelengths and higher values of d/Λ. Especially, the values of the effective refractive index, effective mode area, dispersion, and confinement loss are strongly influenced by the filling factor and the lattice constant. Optimal structures are the key factors for supercontinuum generation.

Funding statement

This research is funded by Vietnam's Ministry of Education and Training under grant number B2021-DHH-08.

References

1. Yeh P, Yariv A, Marom E. Theory of Bragg fiber. Journal of the Optical Society of America. 1978;68(9):1196-5.
2. Knight JC, Birks TA, Russell PSJ, Atkin DM. All-silica single-mode optical fiber with photonic crystal cladding. Optics Letters. 1996;21(19):1547-2.
3. Sinha RK, Varshney SK. Dispersion properties of photonic crystal fibers. Microwave and Optical Technology Letters. 2003;37:129-132.
4. Maji PS, Roy Chaudhuri P. Supercontinuum generation in ultra-flat near zero dispersion PCF with selective liquid infiltration. Optik. 2014;125(20):5986-92.
5. Lin-Ping S, Wei-Ping H, Shui-Sheng J. Design of photonic crystal fibers for dispersion-related

pISSN 1859-1388
eISSN 2615-9678

applications. Journal of Lightwave Technology. 2003;21(7):1644-1651.

6. Ferrando A, Silvestre E, Miret JJ, Andrés P. Nearly zero ultraflattened dispersion in photonic crystal fibers. Optics Letters. 2000;25(11):790-2.
7. Ferrando A, Silvestre E, Andrés P, Miret JJ, Andrés MV. Designing the properties of dispersion-flattened photonic crystal fibers. Optics Express. 2001;9(13):687-97.
8. Saitoh K, Koshiba M, Hasegawa T, Sasaoka E. Chromatic dispersion control in photonic crystal fibers: application to ultra-flattened dispersion. Optics Express. 2003;11(8):843-52.
9. Poletti F, Finazzi V, Monro TM, Broderick NGR, Tse V, Richardson DJ. Inverse design and fabrication tolerances of ultra-flattened dispersion holey fibers. Optics Express. 2005;13(10): 3728-36.
10. Huttunen A, Törmä P. Optimization of dual-core and microstructure fiber geometries for dispersion compensation and large mode area. Optics Express. 2005;13(2):627-35.
11. Saitoh K, Koshiba M. Single-polarization single-mode photonic crystal fibers. IEEE Photonics Technology Letters. 2003;15(10):1384-6.
12. Kubota H, Kawanishi S, Koyanagi S, Tanaka M, Yamaguchi S. Absolutely single polarization photonic crystal fiber. IEEE Photonics Technology Letters. 2004;16(1):182-4.
13. Dobb H, Kalli K, Webb DJ. Temperature-insensitive long period grating sensors in photonic crystal fibre. Electronics Letters. 2004;40(11):657-8.
14. Dong X, Tam HY, Shum P. Temperature-insensitive strain sensor with polarization-maintaining photonic crystal fiber based Sagnac interferometer. Applied Physics Letters. 2007;90(15):151113.
15. Hartung A, Heidt AM, Bartelt H. Design of all-normal dispersion microstructured optical fibers for pulse-preserving supercontinuum generation. Optics Express. 2011;19(8):7742-9.
16. Xueming L, Xiaoqun Z, Xiufeng T, Junhong N, Jianzhong H, Teck Yoong C, et al. Switchable and tunable multiwavelength erbium-doped fiber laser with fiber Bragg gratings and photonic crystal fiber. IEEE Photonics Technology Letters. 2005;17(8):1626-8.
17. Agrawal A, Kejalakshmy N, Chen J, Rahman BMA, Grattan KTV. Golden spiral photonic crystal fiber: polarization and dispersion properties. Optics Letters. 2008;33(22):2716-8.
18. Stefaniuk T, Le Van H, Pniewski J, Cao Long V, Ramaniuk A, Grajewski K, et al. Dispersion engineering in soft glass photonic crystal fibers infiltrated with liquids. Event: 16th Conference on Optical Fibers and Their Applications, Lublin and Naleczow, Poland. 2015;9816.
19. Xuan KD, Van LC, Long VC, Dinh QH, Van Mai L, Trippenbach M, et al. Influence of temperature on dispersion properties of photonic crystal fibers infiltrated with water. Optical and Quantum Electronics. 2017;49:87.
20. Van Lanh C, Hoang VT, Long VC, Borzycki K, Xuan KD, Quoc VT, et al. Optimization of optical properties of photonic crystal fibers infiltrated with chloroform for supercontinuum generation. Laser Physics. 2019;29(7):075107.
21. Van Le H, Cao VL, Nguyen HT, Nguyen AM, Buczyński R, Kasztelanic R. Application of ethanol infiltration for ultra-flattened normal dispersion in fused silica photonic crystal fibers. Laser Physics. 2018;28(11):115106.
22. Fatome J, Fortier C, Nguyen TN, Chartier T, Smektala F, Messaad K, et al. Linear and Nonlinear Characterizations of Chalcogenide Photonic Crystal Fibers. Journal of Lightwave Technology. 2009;27(11):1707-15.
23. Vigreux-Bercovici C, Ranieri V, Labadie L, Broquin JE, Kern P, Pradel A. Waveguides based on $Te_2As_3Se_5$ thick films for spatial interferometry. Journal of Non-Crystalline Solids. 2006;352(23-25):2416-9.
24. Price JHV, Monro TM, Ebendorff-Heidepriem H, Poletti F, Horak P, Finazzi V, et al. Mid-IR Supercontinuum Generation from Nonsilica Microstructured Optical Fibers. IEEE Journal of Selected Topics in Quantum Electronics. 2007;13(3):738-49.
25. Domachuk P, Wolchover NA, Cronin-Golomb M, Wang A, George AK, Cordeiro CMB, et al. Over 4000 nm Bandwidth of Mid-IR Supercontinuum Generation in sub-centimeter Segments of Highly Nonlinear Tellurite PCFs. Optics Express. 2008; 16(10):7161-8.
26. Ta'eed VG, Shokooh-Saremi M, Fu L, Moss DJ, Rochette M, Littler ICM, et al. Integrated all-optical pulse regenerator in chalcogenide waveguides. Optics Letters. 2005;30(21):2900-2.
27. Pelusi MD, Luan F, Magi E, Lamont MRE, Moss DJ, Eggleton BJ, et al. High bit rate all-optical signal

processing in a fiber photonic wire. Optics Express. 2008;16(15):11506-12.

28. Varshney SK, Saitoh K, Iizawa K, Tsuchida Y, Koshiba M, Sinha RK. Raman amplification characteristics of As_2Se_3 photonic crystal fibers. Optics Letters. 2008;33(21):2431-3.
29. Fu LB, Rochette M, Ta'eed VG, Moss DJ, Eggleton BJ. Investigation of self-phase modulation based optical regeneration in single mode As_2Se_3 chalcogenide glass fiber. Optics Express. 2005;13(19):7637-44.
30. Florea C, Bashkansky M, Dutton Z, Sanghera J, Pureza P, Aggarwal I. Stimulated Brillouin scattering in single-mode As_2S_3 and As_2Se_3 chalcogenide fibers. Optics Express. 2006;14(25):12063-70.
31. Dabas B, Sinha RK. Dispersion characteristic of hexagonal and square lattice chalcogenide As_2Se_3 glass photonic crystal fiber. Optics Communications. 2010;283(7):1331-7.
32. Su H, Zhang Y, Ma K, Zhao Y, Wang J. High-temperature sensor based on suspended-core microstructured optical fiber. Optics Express. 2019;27(15):20156-64.
33. Rim Cherif , Mourad Zghal. Ultrabroadband, Midinfrared Supercontinuum Generation in Dispersion Engineered As_2Se_3-Based Chalcogenide Photonic Crystal Fibers. International Journal of Optics. 2013;2013:1-5.
34. Li F, He M, Zhang X, Chang M, Wu Z, Liu Z, et al. Elliptical As_2Se_3 filled core ultra-high-nonlinearity and polarization-maintaining photonic crystal fiber with double hexagonal lattice cladding. Optical Materials. 2018;79:137-46.
35. Mohsin KM, Alam MS, Hasan DMN, Hossain MN. Dispersion and nonlinearity properties of a chalcogenide As_2Se_3 suspended core fiber. Applied Optics. 2011;50(25);E102-E7.
36. Lumerical Eigenmode Expansion (EME) Solver, https://www.lumerical.com/tcad products/mode/EME, accessed 29 August (2016).
37. Cherif R, Ben Salem A, Zghal M, Besnard P, Chartier T, Brilland L, et al. Highly nonlinear As_2Se_3-based chalcogenide photonic crystal fiber for midinfrared supercontinuum generation. Optical Engineering. 2010;49(9):095002.